PROCEEDINGS OF SCIENCE

Baryon interactions from lattice QCD with physical masses – Overview and $S = 0, -4$ sectors –

Takumi Doi[*,a] **Sinya Aoki,**[abc] **Shinya Gongyo,**[ad] **Tetsuo Hatsuda,**[ae] **Yoichi Ikeda,**[af] **Takashi Inoue,**[ag] **Takumi Iritani,**[a] **Noriyoshi Ishii,**[af] **Takaya Miyamoto,**[ab] **Keiko Murano,**[af] **Hidekatsu Nemura,**[ac] **and Kenji Sasaki**[ab]

[a] *Theoretical Research Division, Nishina Center, RIKEN, Wako 351-0198, Japan*
[b] *Yukawa Institute for Theoretical Physics, Kyoto University, Kyoto 606-8502, Japan*
[c] *Center for Computational Sciences, University of Tsukuba, Ibaraki 305-8571, Japan*
[d] *CNRS, Laboratoire de Mathématiques et Physique Théorique, Universitéde Tours, 37200 France*
[e] *iTHEMS Program and iTHES Research Group, RIKEN, Wako 351-0198, Japan*
[f] *Research Center for Nuclear Physics (RCNP), Osaka University, Osaka 567-0047, Japan*
[g] *Nihon University, College of Bioresource Sciences, Kanagawa 252-0880, Japan*
E-mail: doi@ribf.riken.jp

Nuclear forces and hyperon forces are studied by lattice QCD. Simulations are performed with (almost) physical quark masses, $m_\pi \simeq 146$ MeV and $m_K \simeq 525$ MeV, where $N_f = 2+1$ nonperturbatively $\mathcal{O}(a)$-improved Wilson quark action with stout smearing and Iwasaki gauge action are employed on the lattice of $(96a)^4 \simeq (8.1\text{fm})^4$ with $a^{-1} \simeq 2.3$ GeV. In this report, we give the overview of the theoretical framework and present the numerical results for two-nucleon forces ($S = 0$) and two-Ξ forces ($S = -4$). Central forces are studied in ${}^1S_0$ channel, and central and tensor forces are obtained in ${}^3S_1$-${}^3D_1$ coupled channel analysis.

34th annual International Symposium on Lattice Field Theory
24-30 July 2016
University of Southampton, UK

[*]Speaker.

© Copyright owned by the author(s) under the terms of the Creative Commons Attribution-NonCommercial-NoDerivatives 4.0 International License (CC BY-NC-ND 4.0).

arXiv:1702.01600v2 [hep-lat] 28 Feb 2017

1. Introduction

One of the most challenging issues in particle and nuclear physics is to unravel the origin of baryon forces based on the fundamental theory, quantum chromodynamics (QCD). The precise information on nuclear and hyperon forces serve as the key ingredients to calculate properties of nuclei and dense matter and the structure of neutron stars. While so-called realistic nuclear forces have been obtained using experimental scattering phase shifts, their connection to QCD is yet to be established. Hyperon forces suffer from large uncertainties since scattering experiments with hyperon(s) are very difficult due to the short life time of hyperons. Under these circumstances, it is most desirable to carry out the first-principles calculations of baryon forces by lattice QCD.

We study baryon forces using a novel theoretical framework, HAL QCD method, in which the interaction kernels (so-called "potentials") are determined from Nambu-Bethe-Salpeter (NBS) correlators on a lattice [1, 2, 3]. (For the application of obtained lattice baryon forces to the equation of state of dense matter, the structure of neutron stars and the properties of nuclei, see Refs. [4, 5].) The significant advantage of HAL QCD method over the traditional approach (so-called "direct" calculations [6, 7, 8]) is that the baryon-baryon interactions can be extracted without relying on the ground state saturation [2]. In fact, since typical excitation energy in multi-baryon systems is one to two orders of magnitude smaller than $\mathcal{O}(\Lambda_{\rm QCD})$ due to the existence of elastic excited states, the results from the "direct" method [6, 7, 8], which rely on the ground state saturation, become generally unreliable [9, 10].

In this paper, we report the latest lattice QCD results for the baryon forces obtained at (almost) physical quark masses, updating our previous results [11]. We first give a brief overview of the theoretical framework and then present numerical results for two-Ξ ($\Xi\Xi$) forces ($S = -4$) and two-nucleon (NN) forces ($S = 0$) in parity-even channel. Central forces are extracted in $^1S_0$ channel, and central and tensor forces are obtained in $^3S_1$-$^3D_1$ coupled channel analysis. The results for other baryon forces in the same lattice setup are presented in Refs. [12].

2. Formalism

The key quantity in the HAL QCD method is the equal-time NBS wave function. In the case of a NN system, for instance, it is defined by $\phi_W^{NN}(\vec{r}) \equiv 1/Z_N \cdot \langle 0|N(\vec{r},0)N(\vec{0},0)|NN,W\rangle_{\rm in}$, where N is the nucleon operator with its wave-function renormalization factor $\sqrt{Z_N}$ and $|NN,W\rangle_{\rm in}$ denotes the asymptotic in-state of the NN system at the total energy of $W = 2\sqrt{k^2+m_N^2}$ with the asymptotic momentum k, and we consider the elastic region, $W < W_{\rm th} = 2m_N + m_\pi$. The most important property of the NBS wave function is that the asymptotic behavior at $r \equiv |\vec{r}| \to \infty$ is given by $\phi_W^{NN}(\vec{r}) \propto \sin(kr - l\pi/2 + \delta_W^l)/(kr)$, where δ_W^l is the scattering phase shift with the orbital angular momentum l. Exploiting this feature, one can define (non-local) NN potential, $U^{NN}(\vec{r},\vec{r}')$, which is faithful to the phase shifts through the Schrödinger equation [1, 2, 3], $(E_W^{NN} - H_0)\phi_W^{NN}(\vec{r}) = \int d\vec{r}' U^{NN}(\vec{r},\vec{r}')\phi_W^{NN}(\vec{r}')$, where $H_0 = -\nabla^2/(2\mu)$ and $E_W^{NN} = k^2/(2\mu)$ with the reduced mass $\mu = m_N/2$. It has been also proven that $U^{NN}(\vec{r},\vec{r}')$ can be constructed as to be energy-independent [1, 3].

Generally speaking, the NBS wave function can be extracted from the four-point correlator, $G^{NN}(\vec{r},t) \equiv \sum_{\vec{R}} \langle 0|(N(\vec{R}+\vec{r})N(\vec{R}))(t)\ \overline{(NN)}(t=0)|0\rangle$, by isolating the contribution from each energy eigenstate (most typically by the ground state saturation with $t \to \infty$). Such a procedure, however, is practically almost impossible, due to the existence of nearby elastic scattering states. In

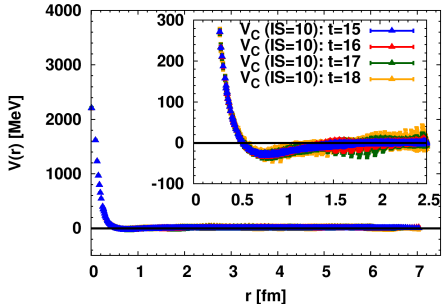

Figure 1: $\Xi\Xi$ central force $V_C(r)$ in ${}^1S_0$ $(I=1)$ channel obtained at $t = 15-18$.

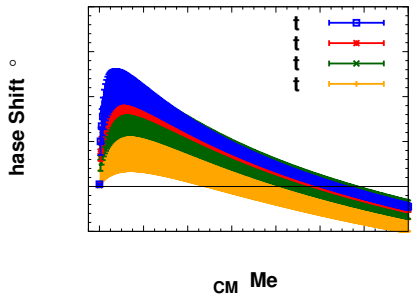

Figure 2: Phase shifts in $\Xi\Xi({}^1S_0)$ $(I=1)$ channel obtained at $t = 15-18$.

fact, the typical excitation energy is as small as $\mathcal{O}(1)-\mathcal{O}(10)$ MeV, which is estimated by the empirical binding energies and/or the discretization in spectrum by the finite volume, $\sim (2\pi/L)^2/m_N$. Correspondingly, ground state saturation requires $t \gtrsim \mathcal{O}(10)-\mathcal{O}(100)$ fm, which is far beyond reach considering that signal/noise is exponentially suppressed in terms of t.

Recently, the breakthrough on this issue was achieved by the time-dependent HAL QCD method [2]. The crucial point is that, since $U^{NN}(\vec{r},\vec{r'})$ is energy-independent, one can extract the signal thereof even from elastic excited states. More specifically, the following "time-dependent" Schrödinger equation holds even without the ground state saturation,

$$\left(-\frac{\partial}{\partial t}+\frac{1}{4m_N}\frac{\partial^2}{\partial t^2}-H_0\right)R^{NN}(\vec{r},t)=\int d\vec{r'}U^{NN}(\vec{r},\vec{r'})R^{NN}(\vec{r'},t), \tag{2.1}$$

where $R^{NN}(\vec{r},t)\equiv G^{NN}(\vec{r},t)e^{2m_N t}$. While it is still necessary to suppress the contaminations from inelastic states, it can be fulfilled by much easier condition, $t \gtrsim (W_{\rm th}-W)^{-1} \sim \mathcal{O}(1)$ fm. This is in contrast to the direct calculations, which inevitably rely on the ground state saturation. Note that while "plateau-like" structures in the effective energy shifts often appear at $t \sim \mathcal{O}(1)$ fm and are customarily used in the previous direct calculations [6, 7, 8], they cannot be distinguished from the fake plateaux (called "mirage" in Ref. [9]) and thus are generally unreliable [9, 10].

The time-dependent HAL QCD method is also essential to study coupled channel systems. Coupled channel effects play an important role in hyperon forces, e.g., in the ΛN-ΣN system and $\Lambda\Lambda$-$N\Xi$-$\Sigma\Sigma$ system. The master formula for a coupled channel system is given by [13]

$$\left(-\frac{\partial}{\partial t}-H_0^\alpha\right)R^{\alpha\beta}(\vec{r},t)=\sum_\gamma \Delta^{\alpha\gamma}\int d\vec{r'}U^{\alpha\gamma}(\vec{r},\vec{r'})R^{\gamma\beta}(\vec{r'},t), \tag{2.2}$$

where α,β,γ denote labels for channels, $R^{\alpha\beta}$ normalized four-point correlator in α (β) channel at the sink (source), $H_0^\alpha = -\nabla^2/2\mu^\alpha$ with the reduced mass $\mu^\alpha = m_1^\alpha m_2^\alpha/(m_1^\alpha+m_2^\alpha)$, $\Delta^{\alpha\gamma} = e^{(m_1^\alpha+m_2^\alpha)t}/e^{(m_1^\gamma+m_2^\gamma)t}$, and subscripts $1,2$ labels for (two) hadrons in the channel. For simplicity, relativistic correction terms are omitted. The advantage of the coupled channel approach in HAL QCD method is also shown in the study of the tetraquark candidate, $Z_c(3900)$ [14].

The computational challenge in lattice QCD for multi-baryon systems is that enormous computational resources are required for the calculation of correlators. The reasons are that (i) the number of Wick contractions grows factorially with mass number A, and (ii) the number of color/spinor contractions grows exponentially for larger A. On this point, we recently develop a novel algorithm

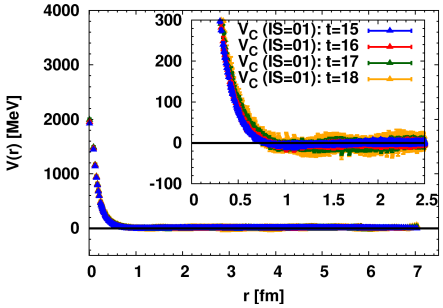

Figure 3: $\Xi\Xi$ central force $V_C(r)$ in ${}^3S_1$-${}^3D_1$ $(I=0)$ channel obtained at $t = 15-18$.

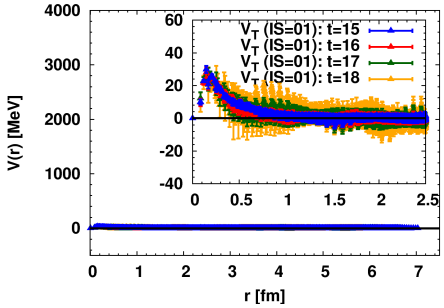

Figure 4: $\Xi\Xi$ tensor force $V_T(r)$ in ${}^3S_1$-${}^3D_1$ $(I=0)$ channel obtained at $t = 15-18$.

called the unified contraction algorithm (UCA), in which two contractions (i) and (ii) are unified in a systematic way [15]. This algorithm significantly reduces the computational cost and play a crucial role in our simulations.

3. Lattice QCD setup

$N_f = 2+1$ gauge configurations are generated on the 96^4 lattice with the Iwasaki gauge action at $\beta = 1.82$ and nonperturbatively $\mathcal{O}(a)$-improved Wilson quark action with $c_{sw} = 1.11$ and APE stout smearing with $\alpha = 0.1$, $n_{\rm stout} = 6$. About 2000 trajectories are generated after the thermalization, and preliminary studies show that $a^{-1} \simeq 2.333$ GeV ($a \simeq 0.0846$ fm) and $m_\pi \simeq 146$ MeV, $m_K \simeq 525$ MeV. The lattice size, $La \simeq 8.1$ fm, is sufficiently large to accommodate two baryons on a box. For further details on the gauge configuration generation, see Ref. [16].

The measurements of NBS correlators are performed at the unitary point, where the block solver [17] is used for the quark propagator and unified contraction algorithm [15] is used for the contraction. The computation for the measurements (including I/O) achieves $\sim 25\%$ efficiency, or ~ 65 TFlops sustained on 2048 nodes of K computer. For two-octet baryon forces, we calculate all 52 channels relevant in parity-even channel. We employ wall quark source with Coulomb gauge fixing, where the periodic (Dirichlet) boundary condition is used for spacial (temporal) directions and forward and backward propagations are averaged to reduce the statistical fluctuations. We pick 1 configuration per each 5 trajectories, and we make use of the rotation symmetry to increase the statistics. The total statistics in this report amounts to 414 configurations $\times$ 4 rotations $\times$ 48 wall sources, binned by 46 configurations. Baryon forces are determined in ${}^1S_0$ and ${}^3S_1$-${}^3D_1$ channels. We perform the velocity expansion [3] in terms of the non-locality of potentials, and obtain the leading order potentials, i.e., central and tensor forces. In this preliminary analysis shown below, the term which corresponds to the relativistic effects ($\partial^2/\partial t^2$-term in Eq. (2.1)) is neglected.

4. $\Xi\Xi$ systems ($S = -4$ channel)

Let us first consider the $\Xi\Xi$ system in ${}^1S_0$ (iso-triplet) channel. This channel belongs to the 27-plet in flavor SU(3) classification as does the $NN({}^1S_0)$ system. Therefore, the $\Xi\Xi({}^1S_0)$ interaction serves as a good "doorway" to probe the $NN({}^1S_0)$ interaction. In addition, since the strong attraction in $NN({}^1S_0)$ makes a "dineutron" nearly bound, it has been attracting interest whether the 27-plet interaction with the SU(3) breaking effects forms a bound $\Xi\Xi({}^1S_0)$ state or not [18].

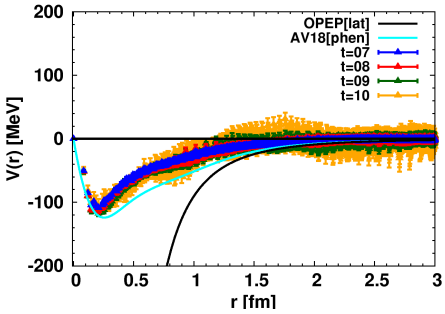

Figure 5: NN tensor force $V_T(r)$ in ${}^3S_1$-${}^3D_1$ ($I = 0$) channel obtained at $t = 7 - 10$, together with bare OPEP and AV18 phenomenological potential.

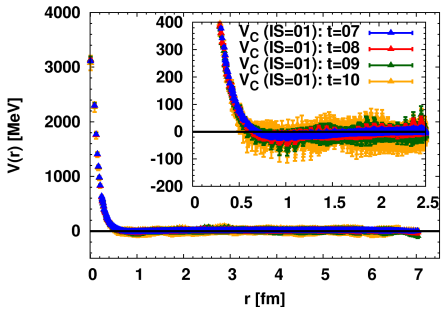

Figure 6: NN central force $V_C(r)$ in ${}^3S_1$-${}^3D_1$ ($I = 0$) channel obtained at $t = 7 - 10$.

In Fig. 1, we show the lattice QCD results for the central force $V_C(r)$ in the $\Xi\Xi({}^1S_0)$ channel. We observe a clear signal of the mid- and long-range attraction as well as the repulsive core at short-range, resembling the phenomenological potential in $NN({}^1S_0)$ system. Within statistical fluctuations, the results are found to be consistent with each other in the range $t = 15 - 18$, which suggests that the contaminations from inelastic excited states are suppressed and higher-order terms in the velocity expansion are small. Shown in Fig. 2 are the corresponding phase shifts in terms of the center-of-mass energy. The results indicate that the interaction is strongly attractive at low energies while it is not sufficient to form a bound $\Xi\Xi({}^1S_0)$ state. It is desirable to examine this observation in experiments by, e.g., heavy-ion collisions.

We next consider the $\Xi\Xi$ system in ${}^3S_1$-${}^3D_1$ (iso-singlet) channel. This channel belongs to the 10-plet in flavor SU(3), a unique representation with hyperon degrees of freedom. By solving the coupled channel Schrödinger equation with NBS correlators, we determine the central and tensor forces. In Figs. 3 and 4, we show the central and tensor forces, respectively. For the central force, we observe the strong repulsive core, which can be understood from the viewpoint of the quark Pauli blocking effect [3, 19]. There also exists an indication of a weak attraction at mid range which may reflect the effect of small attractive one-pion exchange potential (OPEP). We observe that the $\Xi\Xi$ tensor force (Fig. 4) has opposite sign and is weaker compared to the NN tensor forces (Fig. 5). This could be understood by the phenomenological one-boson exchange potentials, where η gives weaker and positive tensor forces and π gives much weaker and negative tensor forces with flavor SU(3) meson-baryon couplings together with F/D ratio by SU(6) quark model. Further studies with larger statistics are currently underway.

5. NN systems ($S = 0$ channel)

Let us begin with the ${}^3S_1$-${}^3D_1$ (iso-singlet) channel. In Fig. 5, we show the tensor force $V_T(r)$ obtained at $t = 7 - 10$. A strong tensor force with the long-range tail is clearly visible. Compared to the lattice tensor forces obtained with heavier quark masses [3], the range of interaction is found to be longer. We also make a qualitative comparison with bare OPEP and the phenomenological tensor force (AV18) in Fig. 5, while a quantitative comparison requires a study in terms of phase shifts which will be presented elsewhere. The tail structures are found to be rather similar among these three potentials. Overall behaviors including the suppression at short-range compare to bare OPEP are also similar between lattice potentials and AV18. Since it is the tensor force which

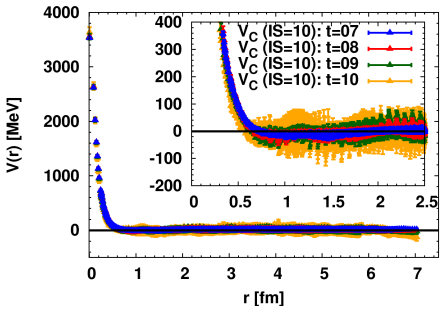

Figure 7: *NN* central force $V_C(r)$ in ${}^1S_0$ $(I = 1)$ channel obtained at $t = 7 - 10$.

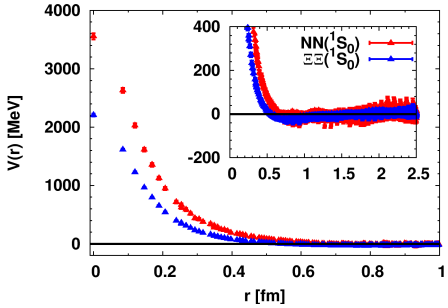

Figure 8: Comparison between central forces in $NN({}^1S_0)$ at $t = 9$ (red) and $\Xi\Xi({}^1S_0)$ at $t = 18$ (blue).

plays the most crucial role in the binding of deuteron, this is a very encouraging result. In order to suppress contaminations from inelastic states, it is desirable to take larger t by increasing the statistics, which is in progress. In Fig. 6, we show the central force $V_C(r)$ in ${}^3S_1$-${}^3D_1$ channel. While the results suffer from much larger statistical fluctuations, the repulsive core at short-range is clearly observed and mid- and long-range attraction is obtained as well.

We then consider the ${}^1S_0$ (iso-triplet) channel. Shown in Fig. 7 is the obtained central force $V_C(r)$ for $NN({}^1S_0)$. As is the case for the central force in ${}^3S_1$-${}^3D_1$ channel, the results suffer from large statistical fluctuations. Yet, the repulsive core at short-range is observed and mid- and long-range attraction is obtained as well. In Fig. 8, we compare $NN({}^1S_0)$ at $t = 9$ (red) and $\Xi\Xi({}^1S_0)$ at $t = 18$ (blue). As noted before, both channels belong to the 27-plet in flavor SU(3) classification, and the difference dictates the SU(3) breaking effect. We observe that the repulsive core in $NN({}^1S_0)$ is more enhanced than $\Xi\Xi({}^1S_0)$, which can be understood from the one-gluon exchange picture.

6. Summary

We have reported the lattice QCD studies for baryon interactions with (almost) physical quark masses, $m_\pi \simeq 146$ MeV and $m_K \simeq 525$ MeV on a large lattice box $(96a)^4 \simeq (8.1\text{fm})^4$. Baryon forces have been calculated from NBS correlators in the (time-dependent) HAL QCD method.

Preliminary results for $\Xi\Xi$ and *NN* interactions have been presented. In the $\Xi\Xi({}^1S_0)$ channel, a strong attraction is obtained, although it is not strong enough to form a bound state. In the $\Xi\Xi$ $({}^3S_1$-${}^3D_1)$ channel, we have observed the strong repulsive core in the central force. Tensor force is found to be weak and have an opposite sign compared to the *NN* tensor force. For *NN* forces, a clear signal for the strong tensor force has been obtained. Repulsive cores as well as mid- and long-range attractions have been observed in central forces in both ${}^1S_0$ and ${}^3S_1$-${}^3D_1$ channels. Repulsive core in $NN({}^1S_0)$ is found to be stronger than $\Xi\Xi({}^1S_0)$. These observations have interesting physical implications from the point of view of quark Pauli blocking effect and phenomenological models of baryon forces. Studies in terms of phase shifts with increased statistics are in progress.

Acknowledgments

We thank members of PACS Collaboration for the gauge configuration generation. The lattice QCD calculations have been performed on the K computer at RIKEN, AICS (hp120281, hp130023, hp140209, hp150223, hp150262, hp160211), HOKUSAI FX100 computer at RIKEN,

Wako (G15023, G16030) and HA-PACS at University of Tsukuba (14a-20, 15a-30). We thank ILDG/JLDG [20] which serves as an essential infrastructure in this study. This work is supported in part by MEXT Grant-in-Aid for Scientific Research (JP15K17667), SPIRE (Strategic Program for Innovative REsearch) Field 5 project and "Priority Issue on Post-K computer" (Elucidation of the Fundamental Laws and Evolution of the Universe).

References

[1] N. Ishii, S. Aoki and T. Hatsuda, Phys. Rev. Lett. **99** (2007) 022001 [nucl-th/0611096]; S. Aoki, T. Hatsuda and N. Ishii, Prog. Theor. Phys. **123** (2010) 89 [arXiv:0909.5585 [hep-lat]].

[2] N. Ishii *et al.* [HAL QCD Collaboration], Phys. Lett. B **712** (2012) 437 [arXiv:1203.3642 [hep-lat]].

[3] Reviewed in S. Aoki *et al.* [HAL QCD Collaboration], Prog. Theor. Exp. Phys. **2012** (2012) 01A105 [arXiv:1206.5088 [hep-lat]].

[4] T. Inoue *et al.* [HAL QCD Collaboration], Phys. Rev. Lett. **111** (2013) 112503 [arXiv:1307.0299 [hep-lat]]; *ibid.,* Phys. Rev. C **91** (2015) 011001 [arXiv:1408.4892 [hep-lat]].

[5] C. McIlroy, C. Barbieri, T. Inoue, T. Doi and T. Hatsuda, arXiv:1701.02607 [nucl-th].

[6] T. Yamazaki, K. i. Ishikawa, Y. Kuramashi and A. Ukawa, Phys. Rev. D **92** (2015) 014501 [arXiv:1502.04182 [hep-lat]] and refereces therein.

[7] K. Orginos *et al.* [NPLQCD Collaboration], Phys. Rev. D **92** (2015) 114512 [arXiv:1508.07583 [hep-lat]] and refereces therein.

[8] E. Berkowitz *et al.* [CalLat Coll.], Phys. Lett. B **765** (2017) 285 [arXiv:1508.00886 [hep-lat]].

[9] T. Iritani *et al.* [HAL QCD Collaboration], JHEP **1610** (2016) 101 [arXiv:1607.06371 [hep-lat]].

[10] T. Iritani [HAL QCD Coll.], PoS LATTICE **2016** (2016) 107 arXiv:1610.09779 [hep-lat]; S. Aoki, T. Doi and T. Iritani [HAL QCD Coll.], PoS LATTICE **2016** (2016) 109 [arXiv:1610.09763 [hep-lat]].

[11] T. Doi *et al.*, PoS LATTICE **2015** (2016) 086 [arXiv:1512.01610 [hep-lat]]; N. Ishii *et al.*, PoS LATTICE **2015** (2016) 087; K. Sasaki *et al.*, PoS LATTICE **2015** (2016) 088; H. Nemura *et al.*, arXiv:1604.08346 [hep-lat].

[12] N. Ishii *et al.*, in these proceedings; K. Sasaki *et al.*, in these proceedings; H. Nemura *et al.*, in these proceedings.

[13] S. Aoki *et al.* [HAL QCD Coll.], Proc. Japan Acad. B **87** (2011) 509 [arXiv:1106.2281 [hep-lat]]. S. Aoki *et al.* [HAL QCD Coll.], Phys. Rev. D **87** (2013) 034512 [arXiv:1212.4896 [hep-lat]].

[14] Y. Ikeda *et al.* [HAL QCD Coll.], Phys. Rev. Lett. **117** (2016) 242001 [arXiv:1602.03465 [hep-lat]].

[15] T. Doi and M. G. Endres, Comput. Phys. Commun. **184** (2013) 117 [arXiv:1205.0585 [hep-lat]].

[16] K.-I. Ishikawa *et al.* [PACS Coll.], PoS LATTICE **2015** (2016) 075 [arXiv:1511.09222 [hep-lat]].

[17] T. Boku *et al.*, PoS LATTICE **2012** (2012) 188 [arXiv:1210.7398 [hep-lat]]; M. Terai *et al.*, IPSJ Transactions on Advanced Computing Systems, Vol.6 No.3 43-57 (Sep. 2013) (in Japanese); Y. Nakamura *et al.*, Comput. Phys. Commun. **183**, 34 (2012) [arXiv:1104.0737 [hep-lat]].

[18] J. Haidenbauer *et al.*, Eur. Phys. J. A **51** (2015) 2, 17 [arXiv:1412.2991 [nucl-th]].

[19] M. Oka, K. Shimizu and K. Yazaki, Nucl. Phys. A **464** (1987) 700.

[20] `"http://www.lqcd.org/ildg"`, `"http://www.jldg.org"`